# Diffusion of multiwall carbon nanotubes (MWCNTs) through a high density polyethylene (HDPE) geomembrane

P. T. Saheli[1], R. K. Rowe[2*], E. J. Petersen[3], D. M. O'Carroll[4]

[1]GeoEngineering Centre at Queen's-RMC, Queen's University, Kingston, Ontario, Canada, K7L 3N6, E: pooneh.saheli@queensu.ca

[2]Professor and Canada Research Chair in Geotechnical and Geoenvironmental Engineering, GeoEngineering Centre at Queen's – RMC, Queen's University, Kingston, Canada, K7L 3N6, E: kerry.rowe@queensu.ca

[3]Material Measurement Laboratory, National Institute of Standards and Technology, Gaithersburg, Maryland 20899, United States, E: elijah.petersen@nist.gov

[4]Department of Civil & Environmental Engineering, University of Western Ontario, London, Ontario, Canada, E: docarrol@uwo.ca

[*] Corresponding author

**Abstract**

The new applications for carbon nanotubes (CNTs) in various fields and consequently their greater production volume have increased their potential release to the environment. Landfills are one of the major locations where carbon nanotubes are expected to be disposed and it is important to ensure that they can limit the release of CNTs. Diffusion of multiwall carbon nanotubes (MWCNTs) dispersed in an aqueous media through a high-density polyethylene (HDPE) geomembrane (as a part of the landfill barrier system) was examined. Based on the laboratory tests, the permeation coefficient was estimated to be less than $5.1 \times 10^{-15}$ m$^2$/s. The potential performance of a HDPE geomembrane and geosynthetic clay liner (GCL) as parts of a composite liner in containing MWCNTs was modelled for six different scenarios. The results suggest that the low value of permeation coefficient of an HDPE geomembrane makes it an effective diffusive barrier for MWCNTs and by keeping the geomembrane defects to minimum during the construction (e.g., number of holes and length of wrinkles) a composite liner commonly used in municipal solid waste landfills will effectively contain MWCNTs.

*Keywords*: Geosynthetics, GMB, permeation coefficient, landfill, municipal solid waste

# 1. Introduction

Carbon nanotubes (CNTs) are tube-shaped carbon structures that can be made of a single layer (single-wall carbon nanotubes, SWCNTs) or several coaxial tubes (multiwall carbon nanotubes, MWCNTs) (Ostiguy et al. 2008). The first synthesized MWCNTs were reported in 1991 (Iijima 1991). MWCNTs range from about 2.5 nm to 50 nm in diameter and from a few tens of nm to several μm in length (Harris 2009, O'Carroll et al. 2013).

Carbon nanotubes have unique electrical, mechanical and thermal characteristics that can be exploited when used in polymer, metal, and ceramic composites or other potential applications (Breuer and Sundararaj 2004; Harris 2009). MWCNTs have the highest stiffness and strength compared to any other material. Their Young's modulus can be up to 1000 GPa (five times higher than steel) and their tensile strength can be as high as 63 GPa (about 50 times higher than steel) (Harris 2009). The combination of these unique mechanical properties with their low density makes carbon nanotubes useful in sports equipment such as tennis rackets and high performance racing bikes and composites with metals such as aluminum or magnesium makes them attractive for the aerospace industry (Breuer and Sundararaj 2004; Harris 2009; Gohardani et al. 2014). Functionalized nanotubes can cross cell membranes, suggesting that in a controlled environment they can be used for drug delivery into cells after assessing their potential toxicity (Harris 2009; Kamalha et al. 2012; Tan et al. 2014).

The innovative applications for CNTs in various fields have led to a rapid increase in their production volume. The world-wide production capacity for CNT estimated to be 430 tonnes/year in 2008 (Mueller and Nowack 2008) and CNT production only in Europe was reported to be 380 tonnes in 2012 (Sun et al. 2014). The increased production of CNTs also raises questions regarding their potential release to the environment (Klaine et al. 2008; Petersen et al. 2011b; Nowack et al. 2013; Petersen et al. 2014) as well as changing their exposure pattern and potentially increasing their potential risks (Environment Canada 2015).

The potential impacts of MWCNTs on soil, sediment, and aquatic organisms have been extensively researched (Kennedy et al. 2008; Petersen et al. 2011b, 2015). In the soil environment, several studies have shown minimal bioaccumulation of MWCNTs by earthworms (Petersen et al. 2008, 2010, 2011a; Li et al. 2013), yet uptake of MWCNTs from soils or water into plants including food crops such as tomatoes has been observed (Khodakovskaya et al. 2011; Larue et al. 2012). Some studies have shown toxic effects from MWCNTs to earthworms (Scott-Fordsmand et al. 2008), while other studies have shown minimal effects on microorganisms or earthworms (Petersen et al. 2009b; Shrestha et al. 2013; Zhang et al. 2014; Oyelami and Semple 2015). MWCNTs in soils may be transported into aquifers where ingestion by humans and subsequent toxicological effects are possible. Thus, studies on their environmental persistence and fate in soils are key topics for additional research (Petosa et al. 2010; Zhang et al. 2011, 2012, 2013).

Using a life-cycle analysis, it was predicted that, in the United States, about 89% of CNT will eventually end up in landfills either directly (77%) and or in ash from incinerator plants (12%) (Gottschalk et al. 2009). In the European Union, it is predicted that 50% of CNTs will be disposed of in landfills (Sun et al. 2014). Whether disposed directly to a landfill or in the ash from an energy-from-waste/incineration facility, the CNT in a polymer or metal matrix can be released into the leachate by matrix degradation, mechanical stresses (abrasion, scratching, sanding), contact with aggressive leachate, and incineration (Lozano and Berge 2012; Petersen et al. 2011b; Nowack et al. 2013).

The barrier system in a modern engineered landfill is designed to limit the release of contaminants to the surrounding environment to concentrations below those allowed by regulations. Composite liners as a part of landfill barrier systems are typically comprised of a high density polyethylene (HDPE) geomembrane (GMB), a geosynthetic clay liner (GCL) or compacted clay liner (CCL), and an attenuation layer (AL) (Rowe et al. 2004; Rowe 2005, 2012b).

As a part of the investigation of CNT mobility in the environment and landfill barrier systems, their migration through porous media has been studied for both SWCNTs (Lecoanet and Wiesner 2004; Jaisi et al. 2008; Tian et al. 2011) and MWCNTs (Liu et al. 2009; Mattison et al. 2011; O'Carroll et al. 2013; Mekonen et al. 2014; Sharma et al. 2014). The results showed that CNTs are mobile in porous media and various factors can affect their mobility. For example, an increase in either pore water velocity, solution ionic strength, or CNT size decreases CNTs mobility and increases their retention, while an increase in either porous media grain size or pH increases their mobility and decreases their retention in the porous media. Transport of SWCNTs through a packed-bed of mixed municipal solid waste has also been investigated, and the results showed the SWCNTs mobility is limited in young waste environments yet increases as the waste matures (Khan et al. 2013).

Diffusive properties of high density polyethylene (HDPE) geomembranes have been studied for chloride (Rowe 2012a) and various aromatic and chlorinated organic compounds in landfill leachate (Park and Nibras 1993; Aminabhavi and Naik 1999; Sangam and Rowe 2001; Joo et al. 2005; Islam and Rowe 2009; McWatters and Rowe 2009, 2010). The diffusion of carbon nanotubes or any other nanoparticle through geomembranes has not yet been reported in the archival literature. Investigating the diffusion of MWCNTs through GMB and their advection through GCL would help assess the performance of a composite liner in controlling the potential release of MWCNTs to the environment from a landfill.

The objectives of this paper are to experimentally evaluate the permeation of MWCNTs dispersed in an aqueous media through an HDPE geomembrane and, based on the measured GMB permeation coefficient, model the potential transfer of MWCNTs through a typical landfill barrier system for six different scenarios.

## 2. Diffusive transport theory

Diffusive transport of a contaminant through a geomembrane (GMB) typically involves three steps (Sangam and Rowe 2001): adsorption, diffusion and desorption. The adsorption (and desorption) of contaminant from (and to) an aqueous phase at a concentration $c_f$, adjacent to a GMB, partitions to the surface of the adjacent GMB at a concentration $c_g$, with the partitioning being controlled by the partitioning coefficient $S_{gf}$ by a relationship analogous to Henry's law (Sangam and Rowe 2001):

$$c_g = S_{gf} c_f \tag{1a}$$

Typically, $S_{gf}$ is deduced at steady state and is given by the ratio of the concentration of the contaminant in the GMB, $c_{gF}$ [ML$^{-3}$], to the concentration in the solution, $c_{fF}$ [ML$^{-3}$] at equilibrium:

$$S_{gf} = c_{gF} / c_{fF} \tag{1b}$$

Diffusion of a contaminant through the GMB due to concentration gradient is usually governed by Fick's first law:

$$f = -D_g \frac{dc_g}{dz} \tag{2}$$

where $f$ is the mass flux [ML$^{-2}$T$^{-1}$], $D_g$ [L$^2$T$^{-1}$] is the diffusion coefficient (which is specific to the geomembrane and the contaminant) and $dc_g/dz$ is the concentration gradient in the GMB [ML$^{-4}$] parallel to the direction of transport. Considering the conservation of mass when the diffusion coefficient is constant, the change in the concentration of the contaminant in the GMB with time $t$, can be described by Fick's second law:

$$\frac{\partial c_g}{\partial t} = D_g \frac{\partial^2 c_g}{\partial z^2} \tag{3}$$

Since the measurement of the concentration of a contaminant of interest in the geomembrane is difficult, Equations (1) and (2) are often combined and allow the calculation of transport in terms of the concentrations in the source and receptor fluid:

$$f = -D_g \frac{dc_g}{dz} = -S_{gf}D_g \frac{dc_f}{dz} = -P_g \frac{dc_f}{dz} \qquad (4)$$

where $P_g$ [$L^2T^{-1}$] is the permeation coefficient and represents the mass transfer across the geomembrane under a unit concentration gradient at steady state (Sangam and Rowe 2001) and is given by:

$$P_g = S_{gf}D_g \qquad (5)$$

## 3. Experimental investigation

### 3.1. Materials and methods

3.1.1. HDPE geomembrane

In landfill applications, a 1.5-mm-thick high density polyethylene (HDPE) is commonly used but given that it was hypothesized that the permeation of MWCNTs would be very slow in these experiments, a much thinner (0.5-mm-thick) GMB (Table 1), the thinnest similar GMB available, was used to allow faster diffusion.

3.1.2. MWCNTs properties and dispersion preparation

The experiments were performed using a MWCNT dispersion. MWCNTs with a purity of more than 95 % by mass were purchased from Cheap Tubes Inc. (Grafton, VT, US). The measured average length and diameter of the same type of MWCNTs from the same manufacturer were previously reported to be 9.5 nm ± 2.4 nm and 0.236 μm ± 0.126 μm (uncertainties are standard

deviation values of length (n=200) and diameter (n=130) measurements), respectively after the functionalization and modification processes described below (O'Carroll et al. 2013).

To prepare the MWCNT dispersion for the experiments, first, they were functionalized (acid treated) to increase their stability in aqueous media by adding surface hydroxyl (-OH) and carboxyl (-COOH) functional groups (Liu et al. 1998). For functionalization, MWCNTs ($\approx$100 mg) were added to a mixture of 3:1 v/v sulfuric acid (12 mL) and nitric acid (4 mL). The mixture was placed in a bath sonicator (Fisher Scientific, FS110) for two hours and then filtered through a 0.45 μm polytetrafluorethylene (PTFE) membrane to separate functionalized MWCNTs and acids. To remove the residual acids on the MWCNTs, the filter was rinsed with boiling deionized water (approximately 2 L) until the pH of the filtrate was around neutral. The filter was placed in a desiccator to dry and then the functionalized MWCNTs were removed from the filter and stored in a glass vial for future use (Petersen et al. 2009a; Mattison et al. 2011).

After functionalization, MWCNTs were dispersed in an aqueous media with ionic strength of 7.5 mmol/L and pH of $\approx$7. The aqueous media was chosen based on the literature review with the priority given to making a stable dispersion rather than mimicking landfill leachate. Stability of CNT dispersions is strongly affected by pH and ionic strength of the aqueous media (Lin et al. 2009; Lin et al. 2010; Saleh et al. 2008). CNTs aggregation and precipitation increases at low pH (e.g., pH <5) (Lin et al. 2009; Zhang et al. 2011). Therefore, a pH value was chosen that was sufficiently high to prevent aggregation and also close to the pH of landfill leachate (which is slightly acidic for young leachate but slightly basic for old leachate). Increasing cations in the aqueous media (i.e., ionic strength) induce CNTs aggregation (Zhang et al. 2011). Hence, to make a stable CNT dispersion for performing the experiments, a low ionic strength (i.e., 7.5 mmol/L) (Mattison et al. 2011) was chosen. This mimics some low ionic strength municipal solid waste (MSW) leachates and is likely to be conservative for high ionic strength MSW leachate but it allowed for the preparation of a stable dispersion for the experiments. Moreover, unlike landfill

leachate, the aqueous media used in these experiments does not contain any organic material such as humic acid or acetic acid to simplify quantifying the CNT concentration in the media. The aqueous media (all references to "aqueous media" in this paper are to this specific media) was made by adding 1.26 mmol/L monosodium phosphate ($NaH_2PO_4·H_2O$), 1.73 mmol/L disodium phosphate ($Na_2HPO_4$) and 1 mmol/L sodium bromide (NaBr) to double deionized water (Mattison et al. 2011). Then, a 250 mL beaker containing 200 mL of the aqueous media was placed in an ice-water bath and ≈5 mg of functionalized MWCNTs were dispersed in the media for one hour using a Cole-Palmer 500-Watt Ultrasonic Homogenizer, 13 mm-diameter ultrasonic probe (Mattison et al. 2011). The MWCNTs dispersion was diluted by adding 300 mL aqueous media. A sufficient volume of MWCNTs dispersed in the aqueous media was prepared to fill the diffusion cells (500 mL in each batch). The initial concentration of the mixed MWCNTs dispersion was ≈ 8.5 mg/L as measured by a total organic carbon analyzer (TOC analyser) as described below.

### 3.1.3. Analytical methods

To quantify the concentration of MWCNTs dispersion samples from the diffusion experiment, two instruments were used: a TOC analyzer and a UV/visible (UV-vis) spectrophotometer.

The TOC analyzer (Shimadzu, TOC-5050A) was used to measure the concentration of total carbon (TC) and inorganic carbon (IC) in the MWCNTs dispersion and the organic carbon (OC) concentration was calculated by subtracting the two numbers for each sample. Given that the MWCNTs had been functionalized by adding surface hydroxyl (-OH) and carboxyl (-COOH) functional groups, the TOC analyzer detected them as organic carbon (OC). The calibration curves for total carbon and inorganic carbon were run daily before analysing the samples. The measured detection limit of the TOC analyser was 0.15 mg/L for organic carbon. The linearity of the TOC analyzer for MWCNT samples was tested and yielded a coefficient of determination of 0.9997.

A scanning UV/vis spectrophotometer (Beckman, DU-520) at wavelength $\lambda = 400$ nm (Liu et al. 2009; Mattison et al. 2011; O'Carroll et al. 2013) was used to measure the absorbance of the

dispersed MWCNT in the test samples. The detection limit for absorbance measurements was 0.004 (≈0.1 mg/L MWCNT) which was calculated using the standard deviation of the measurements of multiple diluted dispersed MWCNTs samples. The linearity of the UV/vis spectrophotometer for MWCNT samples was tested and yielded a coefficient of determination of 1.000. A comparison between the UV/vis spectroscopy results and TOC results yielded a coefficient of determination of 0.9965.

The UV-vis and the TOC analyser provide orthogonal methods to assess the change in the concentration of MWCNTs in the test cells. UV-vis spectroscopy uses a non-destructive method of measurement, and hence it was used more frequently than TOC analysis because the test specimens were returned to the cells after UV-vis measurements to minimize the total sample volume and mass of MWCNTs withdrawn from the cells. Importantly, TOC analysis was used to confirm the UV-vis measurements for every third sampling event. The TOC analyser can reveal more information about what is happening in the diffusion cells (e.g., carbon desorption from the GMB or $CO_2$ dissolution from the air space). Interferences in the sample analysis (i.e., different carbon sources in the cells) can be investigated using TOC analyser by differentiating between organic carbon and inorganic carbon as discussed in Section 4. Measurements from UV-vis did not require corrections for these interferences.

### 3.2. GMB diffusion test

To establish the diffusion coefficient, conventional two-compartment (source and receptor) stainless steel cells (Park et al. 1996; Sangam and Rowe 2001; Joo et al. 2005; Islam and Rowe 2009; McWatters and Rowe 2009, 2010) (Figure 1) were used.

Duplicate diffusion cells were set up with the MWCNTs dispersion in the source chamber and aqueous media (ionic strength of 7.5 mmol/L; pH of ≈7) in the receptor chamber. A 0.5-mm-thick HDPE geomembrane was used to separate the source and the receptor chambers. A blank cell was also set up with aqueous media in both source and receptor chambers and a 0.5-mm-thick HDPE

GMB to separate them. The blank cell was used to monitor any background carbon in the samples or laboratory environment that entered the aqueous media. The cells were sampled after set up (initial concentration) and at regular time intervals to monitor the change in the concentration. To increase the statistical significance and confirm reproducibility of the results a second set of tests including a blank cell and three diffusion cells was started after obtaining the initial results from the duplicate diffusion cells.

To ensure that the MWCNTs remained dispersed during testing, the diffusion cells were sonicated (placed in a Fisher Scientific Ultrasonic Cleaners, FS110, filled with tap water) weekly for half an hour. All the results presented in this paper were obtained after weekly sonication of the cells. The concentration drop in the sources between each two measurements before sonication was less than 15%. By reducing agglomeration using sonication, the MWCNTs were more likely to diffuse (if there was to be diffusion). It also kept them suspended rather than settling to the bottom of the chamber as can happen if they agglomerate to a sufficiently large size. Regular sonication of diffusion cells is considered unlikely to have any adverse effects on GMB properties; to the extent that there is any effect, it is to increase mobility of CNTs by keeping them available for diffusion (if they will diffuse) and hence would be conservative (i.e., the test would tend to overestimate the mobility of the MWCNTs though the GMB).

## 4. Analyses using UV-vis and TOC analyser

TOC analyser results indicated that the carbon concentration in the receptors as well as in the blank cell chambers increased from below the detection limit initially to more than 1 mg/L. To investigate this issue, additional tests were performed at two temperatures (room temperature and 40°C), with different GMB thicknesses (0.5 mm, 1.5 mm, and 2.4 mm), and in different media (double deionized water (DDW) and the aqueous media defined in Section 3.1.2). These test, which are described in more details in the Supplementary Material (carbon desorption test), showed that some carbon from the GMB (likely short chain hydrocarbons/waxes and antioxidants known to be present

11

in the resin) diffused to the surface of the geomembrane, desorbed from the GMB, and dissolved in the media and hence were detected by the TOC analyser and not UV-vis at the wavelength analyzed. The amount of carbon desorbing from the GMB depended on the media in contact with GMB (either double deionized water (DDW) or the aqueous media as defined in Section 3.1.2) as well as temperature, and was proportional to the surface area of the GMB (Supplementary Material Tables S1 and S2). IC desorption was higher in aqueous media than in DDW by a factor of four but it was not significantly affected by the temperature and the GMB thickness. Organic carbon (OC) desorption was not affected by media or GMB thickness at room temperature but it increased at 40°C by 7 to 15 times depending on the media and the GMB thickness (slightly higher in aqueous media and increased with GMB thickness). The ratio of the mass of the desorbed organic carbon at 40°C to the GMB surface area was $3.0\pm0.2$ μg/cm$^2$, $4.8\pm0.6$ μg/cm$^2$, and $5.1\pm0.3$ μg/cm$^2$ for 0.5 mm, 1.5 mm, and 2.4-mm-thick HDPE GMB, respectively (Supplementary Material Table S2; these values are the average of DDW and aqueous media measurements and the uncertainty indicates standard deviation values). The results suggested that aqueous media and increased temperature increased the carbon desorption from the GMB. For the conditions corresponding to those in the diffusion tests, the carbon desorption from the GMB in contact with aqueous media at room temperature was 65 % IC and 35 % OC (Supplementary Material Table S1). Sonicating the diffusion cells could also increase the amount of the desorbed carbon from the GMB in the cells. Another source of the carbon detected in the blank cell and receptors was shown to be $CO_2$ dissolution from the air space formed in the cells due to sampling; dissolved $CO_2$ was in the form of IC. To account for these extra sources of carbon in the samples, the TOC data were corrected by subtracting the measured concentration of TOC in similarly treated blank cell.

For the reasons discussed above, more confidence is placed in the results from the UV-vis and the following discussion will focus on the UV-vis results. However, the trend in the TOC-analyser results was consistent with the findings from the UV-vis (although these results had higher

variability due to the need to make the corrections for measured carbon from sources other than the MWCNTs as discussed above).

## 5. Experiment results and estimation of GMB permeation coefficient and GCL hydraulic conductivity

Samples from the duplicate diffusion cells, analysed using UV-vis, did not show any measurable diffusion or partitioning of MWCNTs to the GMB after about 650 days (Figure 2). The slight change and fluctuation in the data is due to very minor (unquantifiable) MWCNT attachment to the cell walls, sampling septa and surface of the GMB itself observed at the termination of the test. All UV-vis measurements were normalized to the initial source measurements at time zero. A second set of the tests, which ran up to 320 days and included four replicates, confirmed the results of the first set of experiments. There was some fluctuation in the measured concentrations in the source of the diffusion cells but there was no measurable partitioning of MWCNTs in the GMB for any of the four replicates at any time during the test.

Since no partitioning of MWCNTs to the HDPE GMB was observed after 650 days (Figure 2), diffusion coefficient, $D_g$, and partitioning coefficient, $S_{gf}$, cannot be estimated individually but the permeation coefficient, $P_g$ (Equation 5), can be estimated from modelling. From the UV-vis spectroscopy results, the detection limit in the receptor (absorbance of 0.004 equals 1% of the initial source measurement) was used as the upper bound concentration in the receptor after 650 days and then the cells were modelled using the computer code POLLUTE (Rowe and Booker 2004). The model indicated that a permeation coefficient of MWCNTs to the GMB of $P_g = 5.1 \times 10^{-15}$ m$^2$/s (Figure 2) would be required to have a receptor concentration at the detection limit at this time. This value can be regarded as an upper bound and the actual value is likely lower (as could be confirmed by running the test even longer); however, this does give enough information to give conservative estimate of impact for a MSW landfill. This estimated $P_g$ for MWCNTs through HDPE GMB is three to four orders of magnitude lower compared to some other organic compounds

13

such as benzene and DCM (Table 2) which suggests HDPE GMB can be effective in limiting the diffusive release of the examined MWCNTs from a landfill. This difference between permeation coefficients of organic compounds and MWCNTs is likely due to difference in behaviour of dissolved organic compounds and MWCNTs which are in the form of a colloidal dispersion. MWCNTs behaviour is likely similar to dissolved ions like chloride regarding their interaction with water. Negative chloride ions in water are surrounded by polar water molecules which makes it difficult for them to enter non-polar polyethylene structure. Similarly, functionalized MWCNTs (with added –OH and –COOH groups) can form hydrogen bonding with water molecules (Smith et al. 2009) which makes MWCNTs partitioning into HDPE GMB more difficult. The average size of the MWCNT (9.5 nm in diameter and 236 nm in length) is also much larger than organic compounds such as benzene (on the order of 0.1 nm; Vančik 2014) which makes it more difficult for the MWCNTs to diffuse through the GMB. For inorganic contaminants such as $Na^+$, $Cl^-$, and heavy metal salts such as $Zn^{2+}$, $Ni^{2+}$, $Mn^{2+}$, an HDPE geomembrane is an excellent diffusive barrier (Rowe et al. 2004).

The estimated upper bound value for $P_g$ is based on virgin GMB. It would be expected that in a MSW landfill (typical temperature of 30 ºC to 40 ºC, pressure, contact with leachate), physical aging of the GMB would increase crystallinity, and to the extent that this would affect MWCNT diffusion, it is likely to reduce diffusion through the intact GMB with aging (Islam and Rowe 2009). However, as oxidative degradation of the GMB occurs and the liner approaches its service life, the number of holes and leakage would become greater and hence there would be an increase the migration of any MWCNTs that are still suspended in the leachate. Thus the long-term fate of MWCNTs in the landfill leachate may affect their potential to migrate out of a landfill and warrants more investigation.

## 6. Estimation of MWCNTs transfer through landfill barrier system

To investigate the effectiveness of a composite liner in containing MWCNTs based on GMB permeation coefficient estimated by the experiment described above, MWCNTs transfer through a typical composite liner of a hypothetical landfill was modelled using POLLUTE (Rowe and Booker 2004). Two composite liner configurations were considered involving a 1.5-mm-thick HDPE GMB and either (i) a geosynthetic clay liner (GCL), or (ii) a compacted clay liner (CCL). In both configurations the composite liner was underlain by an attenuation layer (AL) resting on a 3 m thick aquifer (Table 3, Figure 3). The thickness of the AL was adjusted (based on the thicknesses of the GCL and CCL) so that the distance from the bottom of the GMB to the aquifer was the same for each configuration and met the minimum distance of 3.75 m required by MOE (1998). The infiltration through the landfill cover was assumed to be 0.15 m/yr (= 4110 liters per hectare per day (lphd)). The leakage through the composite liner was calculated using the parameters in Table 3 and Figure 3 (and Eq. 38 from Rowe 1998) and then it was assumed the difference between the infiltration and the calculated leakage is removed by a leachate collection system.

The estimated permeation coefficient of MWCNTs through the GMB was taken as the upper bound values based on the experimental results (i.e., $P_g = 5.1 \times 10^{-15}$ m$^2$/s; Table 2). The effect of the liner temperature on the permeation coefficient is not considered here.

The transport of MWCNTs through a porous media as a colloidal suspension in water is similar to the conventional mass transport equation (including advection, diffusion) with an extra term related to the mass removal of MWCNTs particles by porous media due to three mechanisms associated with colloid filtration theory: (1) interception after contacting the surface of the soil particles, (2) gravity sedimentation, and (3) diffusion into immobile zones (e.g., into secondary pores or into zones with limited advective flow (Liu et al. 2009; O'Carroll et al. 2013)). Many factors affect these mechanisms such as the size of the MWCNTs and the ionic strength of the aqueous phase. When the ionic strength of the aqueous media decreases, the colloid removal due

to deposition on the soil particles decreases. Smaller MWCNTs remain retained by the soil particles to a greater extent compared to larger MWCNTs because there is a larger range of retention sites available for smaller MWCNTs while larger MWCNTs need larger deposition sites on soil particles surface so there is less retention sites for them. The total number of retention sites in a porous media are finite and these sites will be occupied more quickly if the initial MWCNT concentration and consequently the MWCNT mass available for occupying the sites are higher (O'Carroll et al. 2013). The deposition rate decreases with time as the available sites get blocked (filled/occupied) due to considerable net-repulsive energy barrier between MWCNTs and surface of the soil particles. Due to this net-repulsive electrostatic condition, only a small part of the soil particles surface contributes to MWCNTs deposition (Sasidharan et al. 2014). Another factor that affects the retention of MWCNTs in a porous media is the Brownian motion of MWCNTs (which is greater for smaller particles) which can lead to more collisions of MWCNTs with soil particles and hence greater diffusion into immobile zones of the porous media (O'Carroll et al. 2013). Since there was no data on diffusion coefficients of MWCNTs through GCL, CCL and AL in the literature, it was assumed that these values are similar to the reported values for chloride (Table 3, Figure 3). Two hydraulic conductivity values were used for the GCL ($2.3 \times 10^{-11}$ m/s from Saheli 2016 and $2.0 \times 10^{-10}$ m/s from Rowe and Brachman 2004) to investigate its effect on the performance of the barrier system. While it is likely that MWCNTs would be retarded by the structure of the GCL, in the modelling below, it is conservatively assumed that eventually the retardation capacity would be reached and that MWCNTs would be transported like a conservative species (e.g., chloride).

The initial MWCNTs concentration in the landfill was assumed to be 10 mg/L. The CNT mass in a landfill can be estimated to be 12 g CNT/m$^2$ in US and 4.8 g CNT/m$^2$ in Europe (see Supplementary Material for detailed calculations). Since these values for CNT mass in the landfill are all estimates and are not measured values, to be conservative, the ratio of the mass of MWCNTs per unit volume of waste to the initial concentration was taken to be the same as that for chloride

based on MOE (1998). This assumption yields a CNT mass per unit area of landfill about 16 times higher than what is calculated above for landfills in the US (i.e., 200 $g/m^2$ vs 12 $g/m^2$) (Table 4). The calculated CNT mass in the landfill (i.e., 12 g CNT/ $m^2$) was also used for one case in Scenario 6 (as described below) to illustrate the impact of the CNT mass in the landfill. It was assumed that all CNT mass in the landfill was available to be leached out of the waste and hence available for transport through the composite liner and that it was uniformly distributed. This is a conservative assumption given that release of MWCNTs from composite materials is typically only a small fraction (> 1 %) of the total amount in the nanocomposite after weathering and abrasion (Schlagenhauf et al., 2015).

For each composite liner configuration (either with GCL or CCL, Figure 3), the peak concentration in the aquifer was calculated for each of the six scenarios modelled, viz:

Scenario 1: pure diffusion neglecting the GMB and assuming that there is no leakage through the composite liner;

Scenario 2: pure diffusion through the composite liner considering GMB (a comparison of Scenario 2 with Scenario 1 demonstrates the effectiveness of the GMB as a diffusion barrier for MWCNTs);

Scenario 3: diffusion and leakage through 5 holes/ha in the GMB with no wrinkles (Figure 4a & 4c);

Scenario 4: diffusion and leakage through 5 holes/ha where 1 hole/ha is coincident with a 10 m long wrinkle/ha in the GMB and 4 holes/ha are on planar GMB in direct contact with either GCL or CCL (Figure 4);

Scenario 5: diffusion and leakage through 5 holes/ha where 1 hole/ha is coincident with a 100 m long wrinkle/ha in the GMB and 4 holes/ha are on planar GMB (Figure 4);

Scenario 6: diffusion and leakage through 5 holes/ha where 1 hole/ha is coincident with a 1000 m long wrinkle/ha in GMB and 4 holes/ha are on planar GMB (Figure 4);

No wrinkles were included in the modeling for the first three scenarios. The length of interconnected wrinkles depends on many different factors as discussed in Chappel et al. (2012a). The measured length of the longest interconnected wrinkle in a test site on a sunny summer day for uncovered GMB varied between 80 m/ha to 6,600 m/ha over the course of the day (Chappel et al. 2012a). Thus the length of a winkle that will affect leakage through a composite liner will depend on the time of day that the GMB is covered. To illustrate the effect of this, the impact of wrinkles coincident with holes (see Rowe 1998; 2005; 2012b; Rowe et al. 2012; Chappel et al. 2012a; 2012b) was modelled for three different wrinkle lengths in the second three scenarios.

The concentrations provided in the following are for one set of aquifer properties. The calculated impact would be case specific and would, for example, vary depending on the Darcy flux, thickness and dispersivity in the aquifer. Nevertheless, by keeping one set of aquifer properties and comparing the concentration in the aquifer for the scenarios examined, this study provides important information about the relative release rates and the role of the composite liner in containing MWCNT.

For the pure diffusion Scenarios (1 and 2), it was assumed that the entire infiltration (0.15 m/yr = 4110 lphd) is removed by the leachate collection system, and thus there is no Darcy flux through the composite liner. By ignoring the GMB's diffusive resistance, the peak concentration in the aquifer of about 8% of the initial concentration in the landfill occurred after about 300 years for composite liner with either GCL or CCL (Figure 5). When GMB's diffusive resistance to MWCNTs is considered, transfer through the composite liner is substantially slowed allowing more MWCNTs mass to be removed by leachate collection system; in this scenario, the peak concentration in the aquifer was only 0.4% of the initial concentration in the landfill and occurred after about 500 years. Thus an HDPE GMB can very effectively limit the diffusive transport of MWCNTs and work as a migration barrier when there is no hole and hence no leakage through the GMB.

Scenarios 3 to 6 were investigated, because holes may be present even with strict construction quality assurance for GMB installation (e.g., 2.5 holes/ha to 5 holes/ha, Giroud and Bonaparte 2001; Rowe 2005; 2012b). The calculated leakage through the holes for similar scenarios is larger for composite liners with CCL than that with GCL (Table 5) due to higher GMB/CCL transmissivity (Figure 3; Rowe 2012b). For example, for CCL and GCL configurations ($k_{GCL}$=2.0×10$^{-10}$ m/s) with no wrinkle, the calculated leakage through 5 holes/ha in the CCL configuration is about 180 times higher than that in GCL configuration (2.6 lphd vs. 0.014 lphd). When 1 hole/ha is on a wrinkle, depending on the length of the wrinkle, the leakage is 1.6 to 3 times higher for CCL configuration than those for GCL configuration (Table 5). A decrease in GCL hydraulic conductivity from 2.0×10$^{-10}$ m/s to 2.3×10$^{-11}$ m/s decreased the leakage through the composite liner by more than a factor of three for the configuration examined when there was a wrinkle (Table 5). For the scenarios examined, a maximum of 6.0% of the infiltration leaked through the holes into the subsoil and aquifer (Table 5) and the remainder was collected by the leachate collection system. Advective/diffusive transport of MWCNTs (the governing equations are presented in the Supplementary Material) through the composite liner (Scenarios 3 to 6) was modelled in two different ways:

M1: the easiest method of modelling advective/diffusive transfer of a contaminant was to model both the diffusive properties of the components of the composite liner together with the average Darcy flux (leakage, Table 5) through the entire landfill area; and

M2: a more strictly correct but more time consuming alternative method that was also used (and that is essential for contaminants with very high partitioning coefficient and very low diffusion coefficient such as PCBs (Jones 2016) and PBDEs (Saheli 2016)) that considered diffusion over the entire landfill area but focussed the advective transport over a very limited area associated with the wetted radius (e.g., Rowe 2012b) below the holes or wrinkles affected by a hole (Supplementary Material).

19

The results of these two modeling approaches are compared and discussed.

When the GMB had no wrinkles (Scenario 3), the holes were all in direct contact with either GCL or CCL. In this case, the leakage through a composite liner with GCL was so small (for both hydraulic conductivities considered; Table 5) that diffusion of MWCNTs dominated over advection and the peak concentration in the aquifer was practically identical to that calculated for pure diffusion model (0.4% of the initial concentration in the landfill after 520 years). Modelling the transport through the composite liner using both methods M1 and M2 gave the same results (Table 6, Scenario 3). For a composite liner with CCL, the leakage is higher than with either GCL configuration for a similar scenario due to higher transmissivity between GMB and CCL (Table 5). In this case both diffusion and advection contribute in MWCNTs migration although diffusion still dominates for Scenario 3 (Table 6). Modelling method M2 gives earlier and higher peak concentration in the aquifer compared to method M1 (0.9% of the initial concentration in the landfill after 300 years compared to 0.6% after about 500 years).

When one of the holes was on a wrinkle, the leakage through the composite liner increased significantly as the length of the interconnected wrinkles increased (Table 5). For short wrinkles (e.g., 10 m/ha) the contribution of advection (leakage) was similar to that due to diffusion (Table 6, Scenario 4). In a composite liner with GCL having $k_{GCL} = 2.3 \times 10^{-11}$ m/s, the peak concentration in the aquifer was 0.5% of the initial concentration in the landfill by both methods M1 and M2 but at somewhat different times (520 years for M1 and 470 years for M2; Table 6). Considering a "worst case" GCL with $k_{GCL} = 2 \times 10^{-10}$ m/s, the advection increased by a factor of about 3.7 (Table 5, Scenario 4) but still remained small (i.e., less than that for CCL Scenario 3 with no wrinkle) and the normalized peak concentration ($c_P/c_o$ where $c_o$ is the initial concentration in the landfill) calculated by method M1 remained about the same while that calculated with method M2 increased to about 0.7% (Figure 6a, Table 6, Scenario 4). For a composite liner with a CCL, even with a short (10 m/ha) wrinkle, the leakage was between 3 and 12 times higher than for the two GCLs

(Table 5, Scenario 4) and the method of calculation begins to become important with the normalized peak concentration ($c_p/c_o$) calculated by method M2 being 1.5% compared to 0.7% for method M1 (Figure 6b). Thus, for the case considered here, the focusing of the flow on the discrete location of the wrinkle with a hole is different by a factor of two from that calculated for the same leakage spread uniformly over the base of the landfill when the leakage exceeded about 3 litres per hectare per day (lphd). This conclusion should not be generalized because the permeation coefficient of MWCNTs through the GMB is at least three to four orders of magnitude lower than that for typical organic contaminants considered in landfill design such as benzene and DCM (Table 2) and for those contaminants diffusion would still be dominate over advection (leakage) at flows much larger than 3 lphd. However, for MWCNTs, diffusion through the GMB is so small that even small leakages assume relative importance and only results obtained with method M2 will be discussed for longer wrinkles.

With an increase in the wrinkle length to 100 m/ha (Scenario 5) for MWCNT in a landfill with a composite liner, advection through a hole in a single wrinkle tended to dominate over diffusion through the entire geomembrane in terms of the impact on the aquifer (Table 6, Scenario 5). For Scenario 5 with $k_{GCL} = 2.3 \times 10^{-11}$ m/s, the normalized peak concentration in the aquifer was still relatively small at 1.3% (after 270 years). However, for the worst case Scenario 5 with $k_{GCL} = 2 \times 10^{-10}$ m/s, the normalized peak concentration in the aquifer increased to 4.2% (after 200 years), and for the CCL Scenario 5, to 7.2% after 190 years (Table 6 and Figure 7). Whether these values would be acceptable depends on the source concentration in the landfill and an assessment of an allowable concentration in the aquifer (which will be regulation dependant).

The migration of MWCNTs through the GMB with a 1000 m/ha wrinkle (Scenario 6) is governed by that wrinkle and the normalized values of peak impact (Table 6 and Figure 8) range between 9.5% (after 180 years) for $k_{GCL} = 2.3 \times 10^{-11}$ m/s, 27% (after 120 years) for $k_{GCL} = 2 \times 10^{-10}$ m/s, and 35% (after 110 years) for the CCL case.

The modelling was generally conducted using 200 g/m², but as shown by a comparison of the upper and lower curves for a CCL in Figure 8, the CNT mass has a significant impact. The uppermost curve in Figure 8 for 200 g/m² ($k_{CCL}$=1×10⁻⁹ m/s) has a peak concentration in the aquifer of 35% after 110 years while the lowermost curve for otherwise identical conditions except that it uses the estimate of the CNT mass in US landfills of 12 g/m² (which is about 16 smaller) gives a peak concentration in the aquifer about 6 times lower (5.9% at only 30 years). Thus, the results from the worst case situation vary significantly depending upon the estimated CNT mass in the modelled landfill.

The range of results obtained over the six scenarios and the different composite liner configurations examined, highlight the extremely high effectiveness of an intact geomembrane or even a geomembrane with 5 holes/ha in contact with a good clay liner for limiting the migration of MWCNTs from a simulated MSW landfill. The results focus attention on the leakage that could occur through a hole in a wrinkle of different lengths. For the conditions examined, the results suggest for landfills with MWCNTs, attention needs to be paid to limiting the length of wrinkles especially in cases with a CCL. However, it also important to note that the analyses conducted herein are considered quite conservative. Of particular note is the fact that the migration of MWCNTs through the clay liner and the attenuation layer was considered to be like a conservative contaminant with no filtration. In reality, MWCNTs would not migrate conservatively through but would be subject to filtration (e.g., see Liu et al. 2009; Mattison et al. 2011; O'Carroll et al. 2013) which would substantially slow release into the aquifer. It was shown that there is a log-linear relationship between available deposition sites for MWCNTs and specific surface area of the quartz sand particles (Mattison et al. 2011) which suggests clay particles with their large specific surface area would have huge potential for MWCNTs removal. These issues, especially with respect to clayey soils, require more investigation. What can be concluded from the foregoing discussion is that, if analyses of a real landfill similar to those performed herein indicate that transport through a

composite landfill liner will be largely dominated by diffusion, then the diffusive migration of MWCNTs though the liner is likely to be small. The opposite is not necessary true. If an analysis such as that for Scenario 6 suggests the advection dominates over leakage it does not mean that the impact of MWCNTs will necessarily be unacceptable but it does mean that much greater scrutiny must be given to the assumptions used in the analysis to assess whether in reality there may be an unacceptably high release.

**7. Conclusion**

Diffusion tests were performed with a multiwall carbon nanotubes (MWCNTs) dispersion and an HDPE GMB at room temperature to estimate its permeation coefficient. Parameters derived from this experiment were then used to examine the potential migration of MWCNTs for a MSW landfill for a number of cases. Based on the materials and conditions examined, it is concluded that:

- Based on the detection limit of MWCNTs dispersion in the receptor after about 650 days, the upper bound of the permeation coefficient, $P_g$, of MWCNTs dispersed in an aqueous media through an HDPE GMB was $5.1 \times 10^{-15}$ m$^2$/s.

- The inferred permeation coefficient of MWCNTs through HDPE GMB is three to four orders of magnitude lower than that for many organic compounds considered in landfill design (e.g., benzene, DCM) which implies that an HDPE GMB can be a very effective diffusive barrier to MWCNTs.

- Modelling composite liner configurations involving a GCL or a CCL for a hypothetical MSW landfill based on permeation coefficient from the experiment showed that HDPE GMB could be very effective in containing MWCNTs inside the barrier system providing that leakage through the composite liner is minimized by reducing the number of holes and especially the length of interconnected wrinkles during the construction.

- The data and analysis presented herein represents a screening tool that may be used in design to identify cases where MWCNT are not likely problem as well as those that need much more investigations and possibly more sophisticated methods of analysis.

## 8. Acknowledgment

## Notations

Basic SI units are shown in parentheses.

$c_o$    the contaminant  initial concentration in the landfill (kg/l)
$c_f$    the contaminant concentration in fluid (kg/l)
$c_{fF}$    the contaminant concentration in the aqueous solution at
$c_g$    the contaminant concentration in the geomembrane (kg/l)
$c_{gF}$    the contaminant concentration in the geomembrane at equilibrium(kg/l)

$c_p$    the contaminant  peak concentration in the aquifer (kg/l)

$D_g$    diffusion coefficient of the contaminant with respect to the GMB (m$^2$/s)

$f$    contaminant mass flux (kg/m$^2$/s)

$k$    hydraulic conductivity (m/s)

$q_o$    the infiltration through the landfill cover (m/s)

$P_g$    permeation coefficient (m$^2$/s)

$S_{gf}$    partitioning coefficient (-)

$t$    time (s)

$t_p$    time to the contaminant peak concentration in the aquifer (s)

## Abbreviations

| | |
|---|---|
| AL | Attenuation layer |
| CCL | Compacted clay liner |
| CNT | Carbon nanotube |
| DCM | Methylene chloride |
| DDW | Double deionized water |
| GCL | Geosynthetic clay liner |
| GMB | Geomembrane |
| HDPE | High density polyethylene |
| HP-OIT | High pressure oxidative induction time (T) |
| IC | Inorganic carbon |
| lphd | Liters per hectare per day |
| MOE | Ministry of environment |
| MSW | Municipal solid waste |
| MWCNT | Multiwall carbon nanotube |
| OC | Organic carbon |
| Std-OIT | Standard oxidative induction time (T) |
| SWCNT | Single-wall carbon nanotube |
| TC | Total carbon |
| TOC | Total organic carbon |
| UV-vis | UV/visible spectrophotometer |

## 9. References

Aminabhavi, T. M. and Naik, H. G. (1999). Sorption/desorption, diffusion, permeation and swelling of high density polyethylene geomembrane in the presence of hazardous organic liquids. *Journal of Hazardous Materials,* 64, pp. 251-262.

Breuer, O., Sundararaj, U. (2004). Big Returns From Small Fibers: A Review of Polymer/Carbon Nanotube Composites*, Polymer Composites*, 25(6), 630-645.

Chappel, M. J., Brachman, R. W. I., Take, W. A., Rowe, R. K. (2012a). Large-Scale Quantification of Wrinkles in a Smooth Black HDPE Geomembrane, *Journal of Geotechnical and Geoenvironmental Engineering-ASCE*, 138 (6), 671-679.

Chappel, M.J., Rowe, R.K., Brachman, R.W.I. and Take, W.A. (2012b). "A comparison of geomembrane wrinkles for nine field cases", *Geosynthetics International,* 19(6): 453-469

Environment Canada (2015). *Summary of Risk Assessment Conducted Pursuant to subsection 83(1) of the Canadian Environmental Protection Act, 1999; Significant New Activity No. 17192: Multi-wall carbon nanotubes*.

Ewais, A. M. and Rowe, R. K. (2014). Effects of blown film process on initial properties of HDPE geomembranes of different thicknesses. *Geosynthetics International,* 21(1).

Giroud, J. P., and Bonaparte, R. (2001). Geosynthetics in liquid containing structures. *In Geotechnical and Geoenvironmental engineering handbook*. Kluwer Academic Publishing, Norwell, Mass. pp. 789–824.

Gohardani, O., Elola, M. C., Elizetxea, C. (2014). Potential and prospective implementation of carbon nanotubes on next generation aircraft and space vehicles: A review of current and expected applications in aerospace sciences, *Progress in Aerospace Sciences*, 70, 42–68.

Gottschalk, F., Sonderer, T., Scholz, R. W., Nowack, B. (2009). Modeled environmental concentrations of engineered nanomaterials ($TiO_2$, ZnO, Ag, CNT, Fullerenes) for different regions, *Environmental Science & Technology*, 43(24), 9216-9222.

Gudina, S. and Brachman, R. W. I. (2006). Physical Response of Geomembrane Wrinkles Overlying Compacted Clay. *Journal of Geotechnical and Geoenvironmental Engineering.* (132), 1346-1353.

Harris, P. J. F. (2009). *Carbon Nanotubes Science: Synthesis, Properties and Applications*. Cambridge University Press

Iijima, S. (1991) Helical Microtubules of Graphitic Carbon. *Nature*, 354, pp. 56-58.

Islam, M. Z. and Rowe, R. K. (2009). Permeation of BTEX through Unaged and Aged HDPE Geomembranes. *Journal of Geotechnical and Geoenvironmental Engineering,* 135(8), pp. 1130-1140.

Jaisi, D. P., Saleh, N. B. and Blake, R. E. (2008). Transport of Single-Walled Carbon Nanotubes in Porous Media: Filtration Mechanisms and Reversibility, *Environmental Science and Technology*, 42(22), pp. 8317-8323.

Jones, D. D. (2016) *Containment of PCBs and VOCs using Geosynthetics*, PhD Thesis, Queen's University, Kingston, Ontario, Canada.

Joo, J., Nam, K., and Kim, J. (2005). Estimation of mass transport parameters of organic compounds through high density polyethylene geomembranes using a modifield double-compartment apparatus, *Journal of Environmental Engineering-ASCE*, 131(5), 790-799.

Kamalha, E., Shi, X., Mwasiagi, J. I., Zeng, Y. (2012). Nanotechnology and Carbon Nanotubes; A Review of Potential in Drug Delivery, *Macromolecular Research*, 20 (9), 891-898.

Kennedy, A. J., Hull, M. S., Steevens, J.A., Dontsova, K. M., Chappell, M. A., Gunter, J. C., Weiss, C. A., Jr. (2008). Factors influencing the partitioning and toxicity of nanotubes in the aquatic environment. *Environ. Toxicol. Chem. 27*(9), 1932-1941.

Khan, I. A., Berge, N. D., Sabo-Attwood, T., Ferguson,P. L., Saleh, N. B. (2013). Single-Walled Carbon Nanotube Transport in Representative Municipal Solid Waste Landfill Conditions, Environ Sci Technol, 47, 8425-8433.

Khodakovskaya, M. V., de Silva, K., Nedosekin, D. A., Dervishi, E., Biris, A. S., Shashkov, E. V., Galanzha, E. I., Zharov, V. P. (2011). Complex genetic, photothermal, and photoacoustic analysis of nanoparticle-plant interactions. *Proceedings of the National Academy of Sciences of the United States of America*, 108(3), 1028-1033.

Klaine, S., Alvarez, P., Batley, G., Fernandes, T., Handy, R., Lyon, D., Mahendra, S., McLaughlin, M., and Lead, J. (2008). Nanomaterials in the environment: Behavior, fate, bioavailability, and effects, *Environmental Toxicology and Chemistry*, 27(9), 1825–1851.

Larue, C., Pinault, M., Czarny, B., Georgin, D., Jaillard, D., Bendiab, N., Mayne-L'Hermite, M., Taran, F., Dive, V., Carriere, M. (2012). Quantitative evaluation of multi-walled carbon nanotube uptake in wheat and rapeseed. *J. Hazard. Mater. 227*, 155-163.

Lecoanet, H. F. and Wiesner, M. R. (2004). Velocity Effects on Fullerene and Oxide Nanoparticle Deposition in Porous Media, *Environmental Science and Technology*, 38(16), 4377-4382.

Li, S., Irin, F., Atore, F. O., Green, M. J., Canas-Carrell, J. E. (2013). Determination of multi-walled carbon nanotube bioaccumulation in earthworms measured by a microwave-based detection technique. *Sci. Tot. Environ.*, 445, 9-13.

Lin, D., Liu, N., Yang, K., Zhu, L., Xu, Y., Xing, B. (2009). The effect of ionic strength and pH on the stability of tannic acid-facilitated carbon nanotube suspensions, *Carbon*, 47, 2875-2882.

Lin, D., Liu, N., Yang, Xing, B., Wu, F. (2010). Different stabilities of multiwalled carbon nanotubes in fresh surface water samples, *Environmental Pollution*, 158, 1270–1274.

Liu, J., Rinzler, A. G., Dai, H. J., Hafner, J. H., Bradley, R. K., Boul, P. J., Lu, A., Iverson, T., Shelimov, K., Huffman, C. B., Rodriguez-Macias, F., Shon, Y. S., Lee, T. R., Colbert, D. T., Smalley, R. E. (1998). Fullerene pipes, *Science*, 280 (5367), 1253–1256.

Liu, X. Y., O'Carroll, D. M., Petersen, E. J., Huang, Q. G., Anderson, C. L. (2009). Mobility of multi-walled carbon nanotubes in porous media, *Environmental Science and Technology*, 43 (21), 8153–8158.

Lozano, P. and Berge, N. D. (2012). Single-walled carbon nanotube behavior in representative mature leachate, *Waste Management,* 32, 1699–1711

Mattison, N. T., O'Carroll, D. M., Rowe, R. K., Petersen, E. J. (2011). Impact of Porous Media Grain Size on the Transport of Multi-walled Carbon Nanotubes, *Environmental Science and Technology*, 45: 9765–9775

McWatters, R. S. and Rowe, R. K. (2009). Transport of volatile organic compounds through PVC and LLDPE geomembranes from both aqueous and vapour phases. *Geosynthetics International,* 16(6), p. 468–481.

McWatters, R. S. and Rowe, R. K. (2010). Diffusive Transport of VOCs through LLDPE and Two Coextruded Geomembranes. *Journal of Geotechnical and Geoenvironmental Engineering,* 136(9), pp. 1167-1177.

Mekonen, A., Sharma, P., Fagerlund, F. (2014). Transport and mobilization of multiwall carbon nanotubes in quartz sand under varying saturation. *Environmental Earth Sciences*, 71 (8), pp. 3751–3760.

MOE (1998) Ministry of Environment and Climate Change, Ontario Regulation 232/98, *Landfilling sites, Environmental Protection Act*.

Mueller, N. C. and Nowack, B. (2008). Exposure Modeling of Engineered Nanoparticles in the Environment, *Environmental Science and Technology*, 42(12), 4447-4453.

Nowack, B., David, R. M., Fissan, H., Morris, H., Shatkin, J. A., Stintz, M., Zepp, R., Brouwer, D. (2013). Potential release scenarios for carbon nanotubes used in composites. *Environment International*, 59, 1-11.

O'Carroll, D. M., Liu, X., Mattison, N. T., Petersen, E. J. (2013). Impact of diameter on carbon nanotube transport in sand, *Journal of Colloid and Interface Science*, 390, 96-104.

Ostiguy, C., Soucy, B., Lapointe, G., Woods, C., Ménard, L., Trottier, M. (2008). *Health Effects of Nanoparticles, Studies and Research Projects*, Report R-589, Montréal, IRSST, 114 pages.

Oyelami, A. O., Semple, K. T. (2015) Impact of carbon nanomaterials on microbial activity in soil, *Soil Biology & Biochemistry*, 86, 172-180.

Park, J.K. and Nibras, M. (1993). Mass flux of organic chemicals through polyethylene geomembranes, *Water Environment Research*, 65(3), 227-237

Park, J. K., Sakti, J. P., Hoopes, J. A. (1996). Transport of organic compounds in thermoplastic geomembranes I: mathematical model. *Journal of Environmental Engineering*, 122(9), pp. 800–806.

Petersen, E. J., Akkanen, J., Kukkonen, J. V. K., Weber, W. J., Jr. (2009a). Biological uptake and depuration of carbon nanotubes by Daphnia magna, *Environmental Science and Technology*, *43* (8), pp.2969–2975.

Petersen, E. J., Diamond, S. A., Kennedy, A. J., Goss, G. G., Ho, K., Lead, J., Hanna, S. K., Hartmann, N. B., Hund-Rinke, K., Mader, B., Manier, N., Pandard, P., Salinas, E. R., Sayre, P. (2015). Adapting OECD Aquatic Toxicity Tests for Use with Manufactured Nanomaterials: Key Issues and Consensus Recommendations. *Environ. Sci. Technol.* 49(16), 9532-9547.

Petersen, E. J., Huang, Q. G., Weber, W. J., Jr. (2008). Bioaccumulation of radio-labeled carbon nanotubes by *Eisenia foetida, Environ. Sci. Technol,* 42(8), 3090-3095.

Petersen, E. J., Huang, Q. G., Weber, W. J., Jr. (2010). Relevance of octanol-water distribution measurements to the potential ecological uptake of multi-walled carbon nanotubes, *Environ. Toxicol. Chem,* 29(5), 1106-1112.

Petersen, E. J., Lam, T., Gorham, J. M., Scott, K. C., Long, C. J., Stanley, D., Sharma, R., Liddle, J. A., Pellegrin, B., Nguyen, T. (2014). Methods to assess the impact of UV irradiation on the surface chemistry and structure of multiwall carbon nanotube epoxy nanocomposites, *Carbon*, 69, 194-205

Petersen, E. J., Pinto, R. A., Landrum, P. F., Weber, W. J., Jr. (2009b). Influence of carbon nanotubes on pyrene bioaccumulation from contaminated soils by earthworms, *Environ. Sci. Technol,* 43, (11), 4181-4187.

Petersen, E. J., Pinto, R. A., Zhang, L., Huang, Q. G., Landrum, P. F., Weber, W. J. (2011a). Effects of polyethyleneimine-mediated functionalization of multi-walled carbon nanotubes on earthworm bioaccumulation and sorption by soils, *Environ. Sci. Technol.* 45(8), 3718–3724.

Petersen, E. J., Zhang, L., Mattison, N., O'Carroll, D., Whelton, A., Uddin, N., Nguyen, T., Huang, Q., Henry, T., Holbrook, R. D., Chen, K.L. (2011b). Potential release pathways, environmental fate, and ecological risks of carbon nanotubes, *Environmental Science and Technology,* 45, 9837–9856.

Petosa, A. R., Jaisi, D. P., Quevedo, I. R., Elimelech, M., Tufenkji, N. (2010). Aggregation and deposition of engineered nanomaterials in aquatic environments: Role of physicochemical interactions, *Environ. Sci. Technol,* 44(17), 6532-6549.

Rowe, R. K. (1998). Geosynthetics and the minimization of contaminant migration through barrier systems beneath solid waste, 6th International Conference on Geosynthetics, Atlanta, Georgia USA. 1, 27-103.

Rowe, R. K. (2005). Long-term performance of contaminant barrier systems, 45th Rankine Lecture, *Geotechnique*, 55(9), 631-678.

Rowe, R. K. (2012a). Design and construction of barrier systems to minimize environmental impacts due to municipal solid waste leachate and gas", 3rd Indian Geotechnical Society: Ferroco Terzaghi Oration, *Indian Geotechnical Journal*, 42(4), 223-256.

Rowe, R. K (2012b). Short and long-term leakage through composite liners, The 7th Arthur Casagrande Lecture, *Canadian Geotechnical Journal*, 49(2), 141-169.

Rowe, R. K. and Booker, J. R. (2004). *POLLUTE v.7- 1D Pollutant Migration Through a Non-Homogeneous Soil,* GAEA Environmental Engineering Ltd.

Rowe, R. K. and Brachman, R. W. I. (2004). Assessment of equivalence of composite liners. *Geosynthetics International*, 11(4), 273-286.

Rowe, R. K., Quigley, R. M., Brachman, R. W., Booker, J. R. (2004). *Barrier Systems for Waste Disposal Facilities.* 2nd ed. New York: Spon Press.

Rowe, R.K., Chappel, M.J., Brachman, R.W.I. and Take, W.A. (2012). "Field monitoring of geomembrane wrinkles at a composite liner test site", Canadian Geotechnical Journal, 49(10): 1196-1211.

Saheli, P. T. (2016). *Transport of PBDE, MWCNTs, and BPA (contaminants of emerging concern) through modern landfill liners*, PhD Thesis, Queen's University, Kingston, Ontario, Canada.

Saleh, N. B., Pfefferle, L. D., Elimelech, M. (2008). Aggregation Kinetics of Multiwalled Carbon Nanotubes in Aquatic Systems: Measurements and Environmental Implications, *Environ. Sci. Technol.*, 42, 7963–7969.

Sangam, H. P. and Rowe, R. K. (2001). Migration of dilute aqueous organic pollutants through HDPE geomembranes. *Geotextiles and Geomembranes,* 19, 329-357.

Sasidharan, S., Torkzaban, S., Bradford, S. A., Dillon, P. J., Cook, P. G. (2014). Coupled effects of hydrodynamic and solution chemistry on long-term nanoparticle transport and deposition in saturated porous media, *Colloids and Surfaces A: Physicochemical and Engineering Aspects*, 457, 169–179.

Schlagenhauf L., Kianfar, B., Buerki-Thurnherr, T., Kuo, Y-Y., Wichser, A., Nüesch, F., Wick, P. and Wang, J. (2015). Weathering of a carbon nanotube/epoxy nanocomposite under UV light and in water bath: impact on abraded particles, *Nanoscale*, 7, 18524–18536

Scott-Fordsmand, J. J., Krogh, P. H., Schaefer, M., Johansen, A. (2008). The toxicity testing of double-walled nanotubes-contaminated food to Eisenia veneta earthworms, *Ecotox. Environ. Saf.* 71(3), 616-619.

Sharma, P., Bao, D., Fagerlund, F. (2014). Deposition and mobilization of functionalized multiwall carbon nanotubes in saturated porous media: effect of grain size, flow velocity and solution chemistry. *Environmental Earth Sciences*, 72 (8), pp. 3025–3035.

Shrestha, B., Acosta-Martinez, V., Cox, S. B., Green, M. J., Li, S., Canas-Carrell, J. E. (2013). An evaluation of the impact of multiwalled carbon nanotubes on soil microbial community structure and functioning, *J. Hazard. Mater.,* 261, 188-197.

Smith, B., Wepasnick, K., Schrote, K. E., Cho, H. H., Ball, W. P., Fairbrother, D. H. (2009). Influence of surface oxides on the colloidal stability of multi-walled carbon nanotubes: A structure-property relationship, *Langmuir 25* (17), 9767–9776.

Sun, T. Y., Gottschalk, F., Hungerbühler, K., Nowack, B (2014). Comprehensive probabilistic modelling of environmental emissions of engineered nanomaterials, *Environmental Pollution*, 185, 69-76.

Tan, J. M., Arulselvan, P., Fakurazi, Sh., Ithnin, H., Hussein, M. Z. (2014). A Review on Characterizations and Biocompatibility of Functionalized Carbon Nanotubes in Drug Delivery Design, *Journal of Nanomaterials*

Tian, Y. A., Gao, B., Ziegler, K. J. (2011). High mobility of SDBS-dispersed single-walled carbon nanotubes in saturated and unsaturated porous media, *J. Hazard. Mater.* 186(2-3), 1766-1772.

Vančik, H. (2014) *Basic Organic Chemistry for the Life Sciences*, Springer International Publishing, Switzerland

Zhang, L. J., Hu, C. W., Wang, W. L., Ji, F. N., Cui, Y. B., Li, M. (2014). Acute toxicity of multi-walled carbon nanotubes, sodium pentachlorophenate, and their complex on earthworm Eisenia fetida, Ecotox. Environ. Saf. , 103, 29-35.

Zhang, L. W., Petersen, E. J., Habteselassie, M. Y., Mao, L., Huang, Q. G. (2013). Degradation of multiwall carbon nanotubes by bacteria, *Environ. Pollut.,*181, 335-339.

Zhang, L. W., Petersen, E. J., Huang, Q. G. (2011). Phase distribution of ^{14}C-labeled multiwalled carbon nanotubes in aqueous systems containing model solids: Peat, *Environ. Sci. Technol.*, 45(4), 1356-1362.

Zhang, L. W., Petersen, E. J., Zhang, W., Chen, Y. S., Cabrera, M., Huang, Q. G. (2012). Interactions of C-14-labeled multi-walled carbon nanotubes with soil minerals in water, *Environ. Pollut.,* 166, 75-81.

**Table 1. Properties of HDPE geomembrane manufactured by Solmax International Inc., Quebec, Canada (modified from Ewais and Rowe 2014)**

| Properties | Unit | Value |
|---|---|---|
| Nominal thickness (ASTM D5199) | mm | 0.5 |
| Resin density (ASTM D1505) | g/cm$^3$ | 0.937 |
| GMB density (ASTM D1505) | g/cm$^3$ | 0.947 |
| Std-OIT (ASTM D3895) | min | $175 \pm 3$ |
| HP-OIT (ASTM D5885) | min | $930 \pm 34$ |
| Degree of crystallinity (ASTM793) | % | $52.7 \pm 2.4$ |

**Table 2. Reported $S_{gf}$ and $D_g$ for various contaminants for HDPE geomembrane**

| Compound | $D_g$ (m$^2$/s) | $S_{gf}$ (-) | $P_g$ (m$^2$/s) | Reference |
|---|---|---|---|---|
| Benzene | $3.5 \times 10^{-13}$ | 30 | $1.0 \times 10^{-11}$ | Sangam and Rowe (2001) |
| Dichloromethane | $6.5 \times 10^{-13}$ | 6 | $4.0 \times 10^{-12}$ | Sangam and Rowe (2001) |
| Chloride | ind | ind | $< 4.0 \times 10^{-18}$ | Rowe (2012a) |
| MWCNT | ind | ind | $< 5.1 \times 10^{-15}$ | This study |

ind = indeterminate

**Table 3. Properties of the composite liner examined in landfill modelling**

| Parameter | | Unit | Value |
|---|---|---|---|
| GMB | | | |
| Thickness | $h$ | m | 0.0015 |
| Density | $\rho$ | g/cm$^3$ | 0.946 |
| Permeation coefficient | $P_g$ | m$^2$/yr | $5.6\times10^{-15}$ |
| Attenuation layer (AL) | | | |
| Density | $\rho$ | g/cm$^3$ | 1.9 |
| Diffusion coefficient | $D_e$ | m$^2$/yr | 0.02[b] |
| Hydraulic conductivity | $k$ | m/s | $1.0\times10^{-7}$[b] |
| Porosity | $n$ | - | 0.3[d] |
| Other parameters | | | |
| Dispersivity (all layers) | $\alpha$ | m | 0.4 |
| Leachate head on GMB | $h_w$ | m | 0.3[d] |
| Aquifer velocity | $v_{bin}$ | m/yr | 1[b] |
| Potentiometric level[a] | $h_a$ | m | 3[d] |
| Aquifer thickness | $h_b$ | m | 3[b] |
| Hole radius | $r_o$ | mm | 5.7[b] |
| Wrinkle compressed width | $2b$ | m | 0.1[c] |

[a] Above bottom of the attenuation layer over the aquifer, [b]Rowe and Brachman (2004); [c]Gudina and Brachman (2006) ; [d]Rowe (2012b)

**Table 4. Input data for modelling MWCNTs transfer through landfill barrier system**

| Parameter | Unit | Value |
|---|---|---|

| Landfill length | $L$ | m | 1000 |
|---|---|---|---|
| Landfill width | $W$ | m | 500 |
| Infiltration | $q_o$ | m/yr | 0.15 |
| Waste height | $H_w$ | m | 28 |
| Waste density | $\rho_w$ | kg/m$^3$ | 1000 |
| Reference height of leachate[a] (similar to chloride) | $H_r$ | m | 20 |
| Initial concentration in the landfill | $c_o$ | mg/L | 10 |
| Total mass in waste per unit area[b] | $m_{TC}$ | g/m$^2$ | 200 |

[a] $H_r$ is equal to the mass of contaminant per unit area divided by the initial source concentration (calculation is described in Saheli 2016)

[b] $m_{TC} = H_r \times c_o$

**Table 5. Calculated leakage through a composite liner for cases examined with 5 holes/ha in the GMB (Scenarios 3 to 6), the numbers in parenthesis show the percentage of infiltration leaked through the composite liner into the subsoil and aquifer ($q_o = 0.15$ m$^3$/a/m$^2$ = 4110 lphd), the rest of the infiltration is removed by the leachate collection system**

| Composite liner configuration | Leakage (in litres per hectare per day, lphd) | | | |
|---|---|---|---|---|
| | No Wrinkle | 10 m wrinkle | 100 m wrinkle | 1000 m wrinkle |
| GCL ($k$=2.3×10$^{-11}$ m/s) | 0.014 (<0.001 %) | 0.4 (0.01 %) | 3.9 (0.10 %) | 39.1 (0.95 %) |
| GCL ($k$=2.0×10$^{-10}$ m/s) | 0.014 (<0.001 %) | 1.5 (0.04 %) | 15.3 (0.37 %) | 152.5 (3.7 %) |
| CCL ($k$=1.0×10$^{-9}$ m/s) | 2.6 (0.06 %) | 4.6 (0.11 %) | 26.7 (0.65 %) | 248.5 (6.0 %) |

**Table 6. Calculated normalized peak impact, $c_p/c_o$, and time to peak impact, $t_p$, for MWCNT migration through the composite liners consider with 5 holes/ha ($c_o = 10$ mg/L). Numbers rounded to 2 significant digits. In Method 1 (M1), both advective and diffusive transfer of MWCNTs were modelled together considering the average leakage through the entire landfill area. In Method 2 (M2), advective and diffusive transfer of MWCNTs were modelled separately and the results were superimposed considering the leakage over a very limited area associated with the wetted radius (e.g., Rowe 2012b) below the holes or wrinkles affected by a hole.**

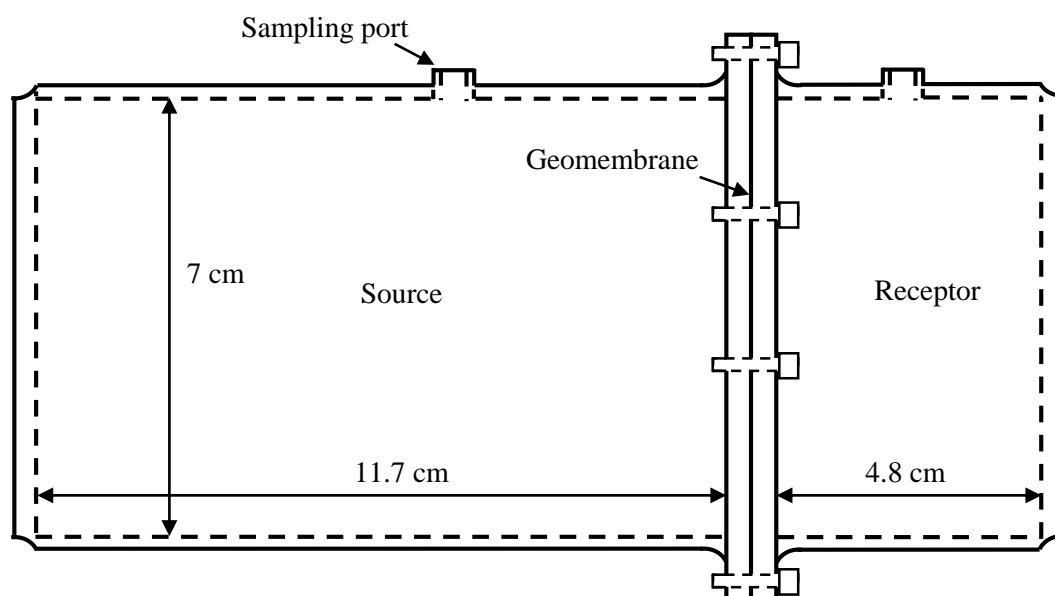| Case | Method | | Scenario 3 | Scenario 4 | Scenario 5 | Scenario 6 |
|------|--------|--|------------|------------|------------|------------|
| GCL $k_{GCL} = 2.3 \times 10^{-11}$ m/s | M1 | $t_p$ (year) | 520 | 520 | 510 | 430 |
| | | $c_p/c_o$ (%) | 0.43 | 0.45 | 0.72 | 5.0 |
| | M2 | $t_p$ (year) | 520 | 470 | 270 | 180 |
| | | $c_p/c_o$ (%) | 0.43 | 0.49 | 1.3 | 9.5 |
| GCL $k_{GCL} = 2.0 \times 10^{-10}$ m/s | M1 | $t_p$ (year) | 520 | 520 | 480 | 280 |
| | | $c_p/c_o$ (%) | 0.43 | 0.53 | 2.0 | 19 |
| | M2 | $t_p$ (year) | 520 | 360 | 200 | 120 |
| | | $c_p/c_o$ (%) | 0.43 | 0.73 | 4.2 | 27 |
| CCL $k_{CCL} = 1.0 \times 10^{-9}$ m/s | M1 | $t_p$ (year) | 530 | 530 | 470 | 220 |
| | | $c_p/c_o$ (%) | 0.59 | 0.74 | 3.3 | 27 |
| | M2 | $t_p$ (year) | 300 | 260 | 190 | 110 |
| | | $c_p/c_o$ (%) | 0.95 | 1.5 | 7.2 | 35 |

**Figure 1. Schematic configuration of a diffusion cell**
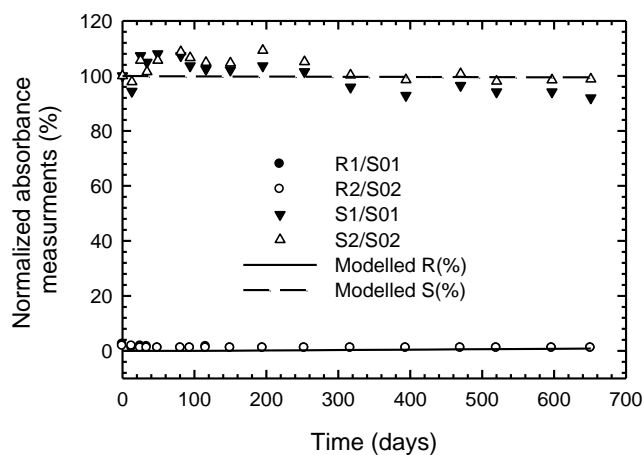


**Figure 2. Normalized UV-vis measurements and numerical model for MWCNTs diffusion through a 0.5-mm-thick HDPE GMB ("Rs" refer to the receptors and "Ss" refer to the sources)**
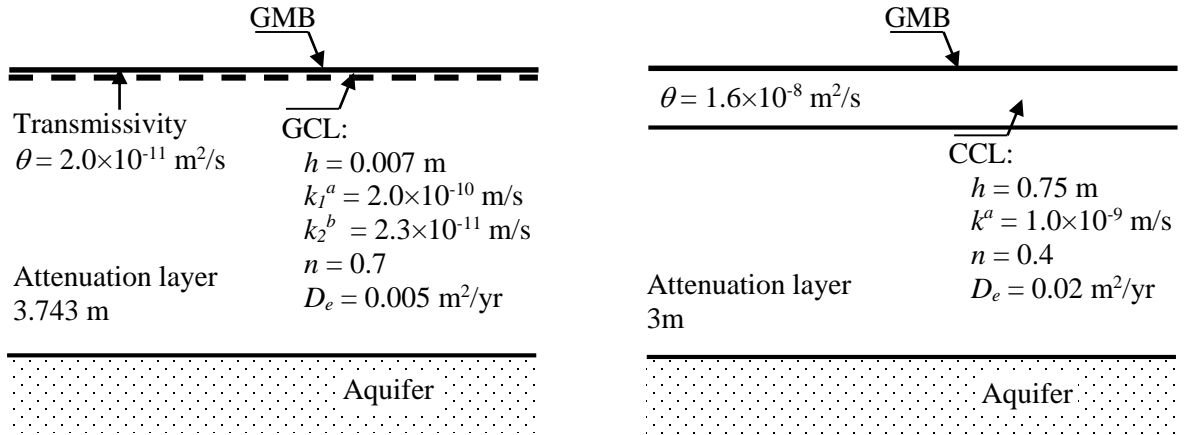
**Figure 3. Typical configurations for a hypothetical landfill barrier system (ᵃRowe and Brachman 2004; ᵇSaheli 2016), ($n$: porosity, $D_e$: diffusion coefficient)**
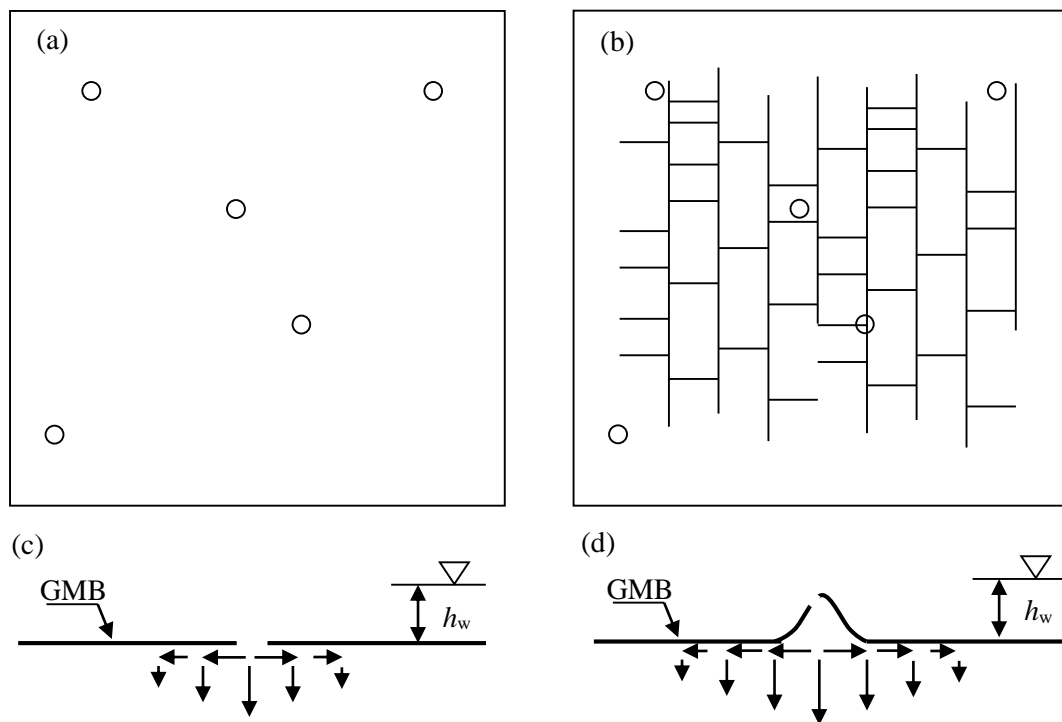


**Figure 4. Schematic of one hectare of the GMB at the bottom of the landfill (a) Scenario 3 with 5 holes/ha and no wrinkle, (b) Scenario 4-6 with 4 holes/ha on the planar GMB and 1 hole/ha on a interconnected wrinkle whose length was 10m, 100, and 1000m for Scenarios 4, 5 & 6 respectively (Scenario 6 shown here), (c) leakage through a hole on the planar GMB and (d) leakage through a hole on a wrinkle ($h_w$: leachate head on geomembrane).**
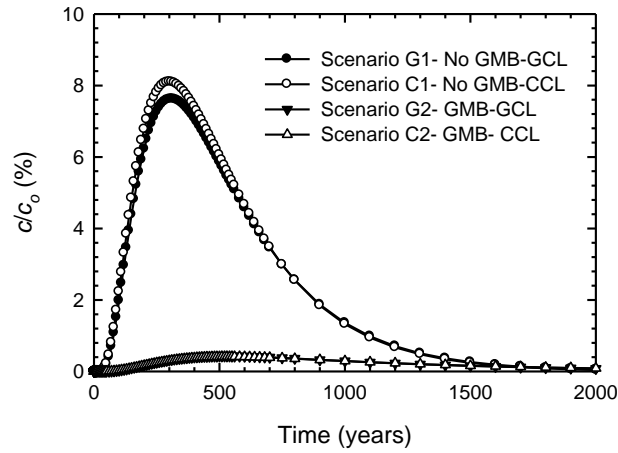
**Figure 5. MWCNTs concentration in the aquifer in pure diffusion scenarios (Scenarios 1 and 2)**
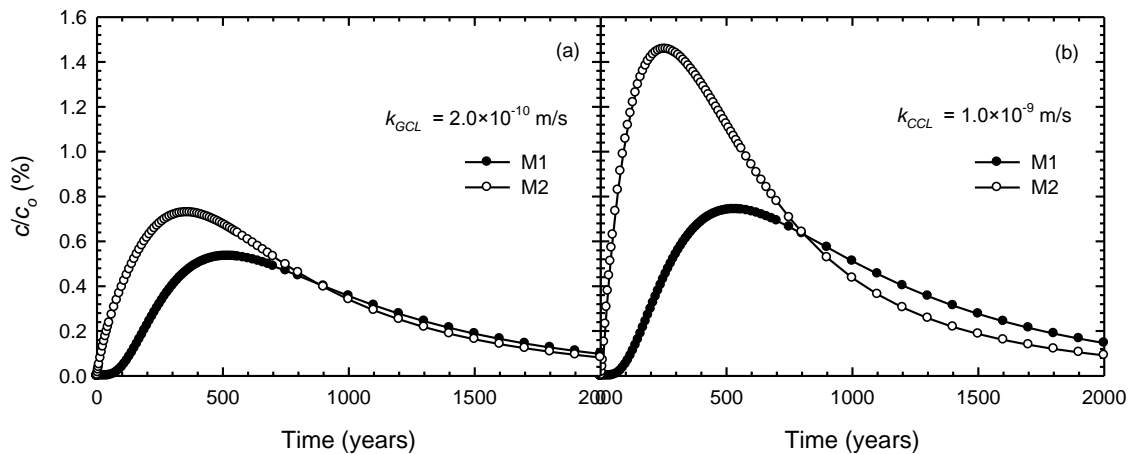


**Figure 6. MWCNT concentration in the aquifer for Scenario 4. In Method 1 (M1), both advective and diffusive transfer of MWCNTs were modelled together considering the average leakage through the entire landfill area. In Method 2 (M2), advective and diffusive transfer of MWCNTs were modelled separately and the results were superimposed considering the leakage over a very limited area associated with the wetted radius (e.g., Rowe 2012b) below the holes or wrinkles affected by a hole.**
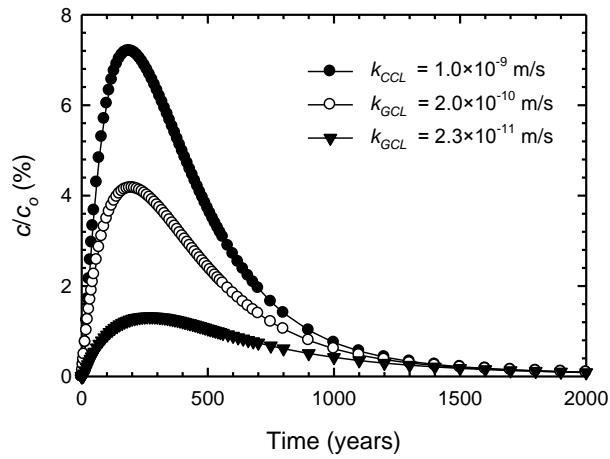
**Figure 7. MWCNT concentration in the aquifer for Scenario 5 (calculated using method M2)**
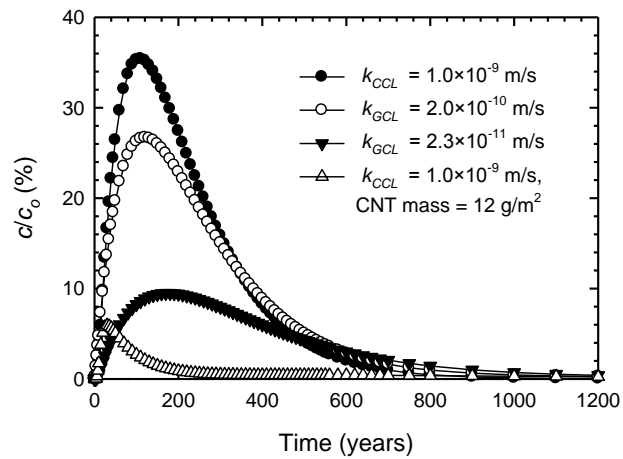


**Figure 8. MWCNT concentration in the aquifer for Scenario 6 with 200 g/m² initial CNT mass in the landfill except for the bottom case where it was assumed that the initial CNT mass was 12 g/m² (all curves calculated using method M2)**